

# COMULTIPLICATION IN LINK FLOER HOMOLOGY AND TRANSVERSELY NON-SIMPLE LINKS

JOHN A. BALDWIN

ABSTRACT. For a word  $w$  in the braid group  $B_n$ , we denote by  $T_w$  the corresponding transverse braid in  $(\mathbb{R}^3, \xi_{rot})$ . We exhibit a map on link Floer homology  $\Phi : HFL^-(m(T_{w\sigma_i})) \rightarrow HFL^-(m(T_w))$  which sends  $\theta(T_{w\sigma_i})$  to  $\theta(T_w)$ , where  $\sigma_i$  is one of the standard generators of  $B_n$ . This gives rise to a “comultiplication” map on link Floer homology, similar in spirit to the map discovered in [2]. We use this to generate infinitely many new examples of prime topological link types which are not transversely simple.

## 1. INTRODUCTION

Transverse knots and links feature prominently in the study of contact 3-manifolds. They arise very naturally – for instance, as binding components of open book decompositions – and can be used to discern important properties of the contact structures in which they sit (see [1, Theorem 1.15] for a recent example). Yet, transverse links, even in the standard tight contact structure,  $\xi_{std}$ , on  $\mathbb{R}^3$ , are notoriously difficult to classify up to transverse isotopy.

A transverse link  $T$  comes equipped with two “classical” invariants which are preserved under transverse isotopy: its topological link type and its self-linking number  $sl(T)$ . A basic question in contact geometry is how to tell, given two transverse representatives,  $T$  and  $T'$ , of some topological link with identical self-linking numbers, whether  $T$  and  $T'$  are transversely isotopic; that is, whether the classical data completely determines the *transverse* link type.

For transverse links with more than one component, it makes sense to refine the notion of self-linking number as follows. Let  $T$  and  $T'$  be two transverse representatives of some  $l$ -component topological link type, and suppose there exist labelings  $T = T_1 \cup \cdots \cup T_l$  and  $T' = T'_1 \cup \cdots \cup T'_l$  of the components of  $T$  and  $T'$  for which  $sl(T_i) = sl(T'_i)$  for each  $i$ . If, in addition,  $sl(T) = sl(T')$ , and there exists a topological isotopy sending  $T$  to  $T'$  which sends  $T_i$  to  $T'_i$  for each  $i$ , then we say that  $T$  and  $T'$  have the same *self-linking data*, and we write  $\mathcal{SL}(T) = \mathcal{SL}(T')$ . We say that a topological link type is *transversely simple* if any two transverse representatives,  $T$  and  $T'$ , which satisfy  $\mathcal{SL}(T) = \mathcal{SL}(T')$  are transversely isotopic. Otherwise, the link type is said to be *transversely non-simple*.

From this point on, we shall restrict our attention to transverse links in the tight rotationally symmetric contact structure,  $\xi_{rot}$ , on  $\mathbb{R}^3$ , which is contactomorphic to  $\xi_{std}$ . There are several well-known examples of knot types which are transversely simple. Among these are the unknot [6], torus knots [8] and the figure eight [9].

---

The author was supported by an NSF Postdoctoral Fellowship and NSF grant number DMS-0635607.

Only recently, however, have knot types been discovered which are not transversely simple. These include a family of 3-braids found by Birman and Menasco [5] using the theory of braid foliations; and the (2,3) cable of the (2,3) torus knot, which was shown to be transversely non-simple by Etnyre and Honda using contact-geometric techniques [10]. Matsuda and Menasco have since identified two explicit transverse representatives of this cabled torus knot which have identical self-linking numbers, but which are not transversely isotopic [15]. Their examples take center stage in Section 5 of this paper.

There has been a flurry of progress in finding transversely non-simple link types in the last couple years, spurred by the discovery of a transverse invariant  $\theta$  in link Floer homology [21]; this discovery, in turn, was made possible by the combinatorial description of  $HFL^-$  found by Manolescu, Ozsváth and Sarkar in [13] (see also [14]). This  $\theta$  invariant is applied in [16] to identify several examples of transversely non-simple links, including the knot  $10_{132}$ . In [23], Vértesi proves a connected sum formula for  $\theta$ , which she weilds to find infinitely many examples of non-prime knots which are transversely non-simple (Kawamura has since proven a similar result without using Floer homology [11]).

Finding infinite families of transversely non-simple *prime* knots is generally more difficult. Using a slightly different invariant, also derived from knot Floer homology, Ozsváth and Stipsicz identify such an infinite family among two-bridge knots [19]. And, most recently, Khandhawit and Ng use the invariant  $\theta$  to construct a 2-parameter infinite family of prime transversely non-simple knots, which generalizes the example of  $10_{132}$  [12].

In this paper, we formulate and apply a strategy for generating a slew of new infinite families of transversely non-simple prime links. This strategy hinges on the “naturalness” results below. For a word  $w$  in the braid group  $B_n$ , we denote by  $T_w$  the corresponding transverse braid in  $(\mathbb{R}^3, \xi_{rot})$ .

**Theorem 1.1.** *There exists a map on link Floer homology,*

$$\Phi : HFL^-(m(T_{w\sigma_i})) \rightarrow HFL^-(m(T_w)),$$

*which sends  $\theta(T_{w\sigma_i})$  to  $\theta(T_w)$ , where  $\sigma_i$  is one of the standard generators of  $B_n$ .*

This theorem implies the existence of a “comultiplication” map on link Floer homology, described in the corollary below.

**Corollary 1.2.** *For any two braid words  $h$  and  $g$  in  $B_n$ , there exists a map,*

$$\mu : HFL^-(m(T_{hg})) \rightarrow HFL^-(m(T_g \# T_h)),$$

*which sends  $\theta(T_{hg})$  to  $\theta(T_g \# T_h)$ .*

One may combine Corollary 1.2 with Vértesi’s result governing the behavior of  $\theta$  under connected sums to conclude the following.

**Corollary 1.3.** *If  $\widehat{\theta}(T_g)$  and  $\widehat{\theta}(T_h)$  are both non-zero, then so is  $\widehat{\theta}(T_{hg})$ , where  $\widehat{\theta}$  is the variant of  $\theta$  in the  $\widehat{HFL}$  version of link Floer homology.*

Below, we sketch one way to use these results to find transversely non-simple links. Start with some  $w_1, w_2 \in B_n$  for which  $T_{w_1}$  and  $T_{w_2}$  are topologically isotopic and have the same

self-linking data, but for which  $\widehat{\theta}(T_{w_1}) = 0$  while  $\widehat{\theta}(T_{w_2}) \neq 0$ , so that  $T_{w_1}$  and  $T_{w_2}$  are not transversely isotopic. Now, choose an  $h \in B_n$  for which  $\widehat{\theta}(T_h) \neq 0$ . Corollary 1.3 then implies that  $\widehat{\theta}(T_{hw_2}) \neq 0$  as well. If one can show that  $\widehat{\theta}(T_{hw_1}) = 0$ , that  $T_{hw_1}$  and  $T_{hw_2}$  still represent the same topological link type, and that  $\mathcal{SL}(T_{hw_1}) = \mathcal{SL}(T_{hw_2})$  (this is automatic if  $T_{hw_1}$  and  $T_{hw_2}$  are knots), then one may conclude that  $T_{hw_1}$  represents a transversely non-simple link type.

An advantage of this approach for generating new transversely non-simple link types from old, over, say, that of [23, 11], is that there is no *a priori* reason to expect that the links so formed are composite. We demonstrate the effectiveness of this approach in Section 5 of this paper. In doing so, we describe an infinite family of prime transversely non-simple link types (half are knots; the other half are 3-component links) which generalizes the (2,3) cable of the (2,3) torus knot. Moreover, it is clear that this example only scratches the surface of the potential of our more general technique.

**Organization.** In the next section, we outline the relationship between grid diagrams, Legendrian links and their transverse pushoffs. In Section 3, we review the grid diagram construction of link Floer homology and describe some important properties of the transverse invariant  $\theta$ . In Section 4, we prove Theorem 1.1 and Corollary 1.2. And, in Section 5, we outline a general strategy for using our comultiplication result to produce new examples of transversely non-simple link types, and we give an infinite family of such examples which are prime.

**Acknowledgements.** I wish to thank Lenny Ng for helpful correspondence. His suggestions were key in developing some of the strategy formulated in Section 5.

## 2. GRID DIAGRAMS, LEGENDRIAN AND TRANSVERSE LINKS

In this section, we provide a brief review of the relationship between Legendrian links in  $(\mathbb{R}^3, \xi_{std})$ , transverse braids in  $(\mathbb{R}^3, \xi_{rot})$  and grid diagrams, largely following the discussion in [12]. For a more detailed account, see [12, 17]. The standard tight contact structure  $\xi_{std}$  on  $\mathbb{R}^3$  is given as

$$\xi_{std} = \ker(dz - ydx).$$

An oriented link  $L \subset (\mathbb{R}^3, \xi_{std})$  is called *Legendrian* if it is everywhere tangent to  $\xi_{std}$ , and *transverse* if it is everywhere transverse to  $\xi_{std}$  such that  $dz - ydx > 0$  along the orientation of  $L$ . Any smooth link can be perturbed by a  $C^0$  isotopy to be Legendrian or transverse. We say that two Legendrian (resp. transverse) links are *Legendrian* (resp. *transversely*) isotopic if they are isotopic through Legendrian (resp. transverse) links.

A Legendrian link  $L$  can be perturbed to a transverse link  $L^+$  by pushing  $L$  in the direction positively transverse to  $\xi_{std}$ .  $L^+$  is called the *positive transverse pushoff* of  $L$ . Legendrian isotopic links give rise to transversely isotopic pushoffs. Conversely, every transverse link is the positive transverse pushoff of some Legendrian link; however, two such Legendrian links need not be Legendrian isotopic. The precise relationship between Legendrian and transverse links is best explained via *front projections*.

The front projection of a Legendrian link is its projection onto the  $xz$  plane. The front projection of a generic Legendrian link has no vertical tangencies and has only semicubical cusps and transverse double points as singularities. Moreover, at each double point, the slope of the overcrossing is more negative than the slope of the undercrossing. See Figure 2.c for the front projection of a right-handed Legendrian trefoil.

The *positive* (resp. *negative*) *stabilization* of a Legendrian link  $L$  along some component  $C$  of  $L$  is the Legendrian link whose front projection is obtained from that of  $L$  by adding a zigzag along  $C$  with downward (resp. upward) pointing cusps. See Figure 1. Two Legendrian links are said to be *negatively stably isotopic* if they are Legendrian isotopic after each has been negatively stabilized some number of times along some of its components. The following theorem implies that the classification of transverse links up to transverse isotopy is equivalent to the classification of Legendrian links up to Legendrian isotopy and negative stabilization.



FIGURE 1. 1.a and 1.b are local pictures of the positive and negative stabilizations, respectively, of a Legendrian link along one of its components  $C$ .

**Theorem 2.1** ([7, 18]). *Two Legendrian links are negatively stably isotopic if and only if their positive transverse pushoffs are transversely isotopic.*

Consider the rotationally symmetric tight contact structure on  $\mathbb{R}^3$  defined by

$$\xi_{rot} = \ker(dz - ydx + xdy).$$

The diffeomorphism of  $\mathbb{R}^3$  given by

$$(1) \quad \phi(x, y, z) = (x, 2y, xy + z)$$

sends  $\xi_{rot}$  to  $\xi_{std}$ . One can define transverse links for  $\xi_{rot}$  in the same way that one does for  $\xi_{std}$ . Since  $\phi$  sends a transverse link in  $(\mathbb{R}^3, \xi_{rot})$  to a transverse link in  $(\mathbb{R}^3, \xi_{std})$ , the study of transverse links in  $(\mathbb{R}^3, \xi_{std})$  is equivalent to that in  $(\mathbb{R}^3, \xi_{rot})$ ; however, the latter is often more convenient, per the following theorem of Bennequin.

**Theorem 2.2** ([3]). *Any transverse link in  $(\mathbb{R}^3, \xi_{rot})$  is transversely isotopic to a closed braid around the  $z$ -axis.*

Theorem 2.2 reduces the study of transverse links to the study of braids. For a braid word  $w \in B_n$ , we let  $T_w$  denote the corresponding transverse braid around the  $z$ -axis. Braid words which are conjugate in  $B_n$  clearly correspond to transversely isotopic links. Recall that, for  $w \in B_n$ , a *positive* (resp. *negative*) *braid stabilization* of  $w$  is the operation which replaces  $w$  by the word  $w\sigma_n$  (resp.  $w\sigma_n^{-1}$ ) in  $B_{n+1}$ . We will also refer to  $T_{w\sigma_n}$  (resp.  $T_{w\sigma_n^{-1}}$ ) as the *positive* (resp. *negative*) *braid stabilization* of the transverse link  $T_w$ . The following theorem makes precise the relationship between braids and transverse links in  $(\mathbb{R}^3, \xi_{rot})$ .

**Theorem 2.3** ([18, 25]). *For  $w \in B_n$  and  $w' \in B_m$ , the transverse links  $T_w$  and  $T_{w'}$  are transversely isotopic in  $(\mathbb{R}^3, \xi_{rot})$  if and only if  $w$  and  $w'$  are related by a sequence of conjugations and positive braid stabilizations and destabilizations.*

In Section 5, we use a braid operation called an *exchange move*. If  $a, b$  and  $c$  in  $B_n$  are words in the generators  $\sigma_2, \dots, \sigma_{n-1}$ , then an exchange move is the operation which replaces the word  $w_1 = a\sigma_1 b\sigma_1^{-1}c$  with the word  $w_2 = a\sigma_1^{-1}b\sigma_1 c$ . An exchange move is actually just a composition of conjugations, one positive braid stabilization and one positive destabilization, and so the link  $T_{w_1}$  is transversely isotopic to  $T_{w_2}$ .

It bears mentioning that the self-linking number of a transverse link admits a nice formulation in the language of braids. If  $\Sigma$  is a Seifert surface for a transverse link  $T$ , then the vector bundle  $\xi_{rot}|_\Sigma$  is trivial and, therefore, has a non-zero section  $v$ . Recall that the *self-linking number* of  $T$  is defined by

$$sl(T) = lk(T, T'),$$

where  $T'$  is a pushoff of  $T$  in the direction of  $v$ . Any two links which are transversely isotopic have identical self-linking numbers. For a word  $w \in B_n$ , the self-linking number of  $T_w$  is given simply by  $a(w) - n$ , where  $a(w)$  is the algebraic length of  $w$ .

In what remains of this section, we describe a relationship between the front diagram of a Legendrian link in  $(\mathbb{R}^3, \xi_{std})$  and a braid representation of its positive transverse pushoff, thought of as a transverse link in  $(\mathbb{R}^3, \xi_{rot})$ . Grid diagrams provide the necessary connection.

A *grid diagram*  $G$  is an  $k \times k$  square grid along with a collection of  $k$   $X$ 's and  $k$   $O$ 's contained in these squares such that every row and column contains exactly one  $O$  and one  $X$  and no square contains both an  $O$  and an  $X$ . See Figure 2.a. We call  $k$  the *grid number* of  $G$ . One can produce an oriented link diagram  $L$  from  $G$  by drawing a horizontal segment from the  $O$ 's to the  $X$ 's in each row and a vertical segment from the  $X$ 's to the  $O$ 's in each column so that the horizontal segments pass over the vertical segments (this is the convention used in [12], and the opposite of the convention in [13]), as in Figure 2.b. By rotating  $L$  45° clockwise, and then smoothing the upward and downward pointing corners and turning the leftward and rightward pointing corners into cusps, one obtains the front projection of a Legendrian link, as in Figure 2.c. Let us denote this Legendrian link by  $L(G)$ .

Alternatively, one can construct a braid diagram from  $G$  by drawing a horizontal segment from the  $O$ 's to the  $X$ 's in each row, as before, and drawing a vertical segment from the  $X$ 's to the  $O$ 's for each column in which the marking  $X$  lies under the marking  $O$ . For those columns in which the  $X$  is above the  $O$ , we draw two vertical segments: one from the  $X$  up to the top of the grid diagram, and the other from the bottom of the grid diagram up to the  $O$ . As before, we require that the horizontal segments pass over the vertical segments. Note that all vertical segments are oriented upwards and that the closure of the diagram we have constructed is a braid. See Figures 2.d and 2.e for an example of this procedure. Let us denote the corresponding braid word by  $w(G)$ , read from the bottom up. The relationship between  $T_{w(G)}$  and  $(L(G))^+$  is expressed in the proposition below.

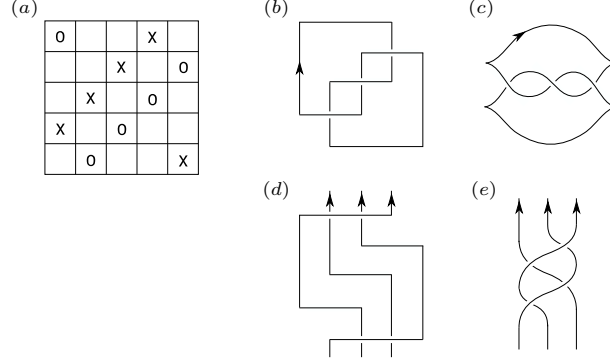


FIGURE 2. In 2.a, a grid diagram  $G$ . In 2.b, the oriented link corresponding to  $G$ . In 2.c, a front projection for the Legendrian link  $L(G)$ . In 2.d and 2.e, the braid corresponding to  $G$ . Here,  $w(G) = \sigma_1\sigma_2\sigma_1\sigma_2$ .

**Proposition 2.4** ([12, Proposition 3]). *The contactomorphism  $\phi$  from  $(\mathbb{R}^3, \xi_{rot})$  to  $(\mathbb{R}^3, \xi_{std})$  defined in Equation (1) sends the transverse link  $T_{w(G)}$  to a link which is transversely isotopic to  $(L(G))^+$ .*

### 3. LINK FLOER HOMOLOGY AND THE TRANSVERSE INVARIANT

In this section, we describe the grid diagram formulation of link Floer homology discovered in [13, 14]. Let  $G$  be a grid diagram for a link  $L$  and suppose that  $G$  has grid number  $k$ . From this point forward, we think of  $G$  as a *toroidal* grid diagram – that is, we identify the top and bottom sides of  $G$  and the right and left sides of  $G$  – so that the horizontal and vertical lines become  $k$  horizontal and  $k$  vertical circles. Let  $\mathcal{O}$  and  $\mathcal{X}$  denote the sets of markings  $\{O_i\}_{i=1}^k$  and  $\{X_i\}_{i=1}^k$ , respectively.

We associate to  $G$  a chain complex  $(CFL^-(m(L)), \partial^-)$  as follows. The generators of  $CFL^-(L)$  are one-to-one correspondences between the horizontal and vertical circles of  $G$ . Equivalently, we may think of a generator as a set of  $k$  intersection points between the horizontal and vertical circles, such that no intersection point appears on more than one horizontal circle or on more than one vertical circle. We denote this set of generators by  $\mathbf{S}(G)$ . Then,  $CFL^-(m(L))$  is defined to be the free  $\mathbb{Z}_2[U_1, \dots, U_k]$ -module generated by the elements of  $\mathbf{S}(G)$ , where the  $U_i$  are formal variables corresponding to the markings  $O_i$ .

For  $\mathbf{x}, \mathbf{y} \in \mathbf{S}(G)$ , we let  $Rect_G(\mathbf{x}, \mathbf{y})$  denote the space of embedded rectangles in  $G$  with the following properties.  $Rect_G(\mathbf{x}, \mathbf{y})$  is empty unless  $\mathbf{x}$  and  $\mathbf{y}$  coincide at  $k - 2$  points. An element  $r \in Rect_G(\mathbf{x}, \mathbf{y})$  is an embedded disk on the toroidal grid  $G$  whose edges are arcs on the horizontal and vertical circles and whose four corners are intersection points in  $\mathbf{x} \cup \mathbf{y}$ . Moreover, we stipulate that if we traverse each horizontal boundary component of  $r$  in the direction specified by the induced orientation on  $\partial r$ , then this horizontal arc is oriented from a point in  $\mathbf{x}$  to a point in  $\mathbf{y}$ . If  $Rect_G(\mathbf{x}, \mathbf{y})$  is non-empty, then it consists of

exactly two rectangles. See Figure 3 for an example. We let  $Rect_G^o(\mathbf{x}, \mathbf{y})$  denote the space of  $r \in Rect_G^o(\mathbf{x}, \mathbf{y})$  for which  $r \cap \mathbb{X} = \text{Int}(r) \cap \mathbf{x} = \emptyset$ .

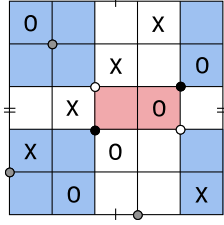


FIGURE 3. A patriotic grid diagram  $G$  for the right-handed trefoil. The generator  $\mathbf{x}$  comprises the black and gray intersection points while  $\mathbf{y}$  comprises the white and gray intersection points.  $Rect_G(\mathbf{x}, \mathbf{y})$  contains the two shaded rectangles in red and blue.

The module  $CFL^-(m(L))$  is endowed with an endomorphism

$$\partial^- : CFL^-(m(L)) \rightarrow CFL^-(m(L)),$$

defined on  $\mathbf{S}(G)$  by

$$\partial^-(\mathbf{x}) = \sum_{\mathbf{y} \in \mathbf{S}(G)} \sum_{r \in Rect_G^o(\mathbf{x}, \mathbf{y})} U_1^{O_1(r)} \cdots U_k^{O_n(r)} \cdot \mathbf{y}.$$

Here,  $O_i(r)$  denotes the number of times the marking  $O_i$  appears in  $r$ . The map  $\partial^-$  is a differential, and, so, gives rise to a chain complex  $(CFL^-(m(L)), \partial^-)$ . The homology of this chain complex,  $HFL^-(m(L)) = H_*(CFL^-(m(L)), \partial^-)$ , is an invariant of the link  $L$ , and agrees with the *link Floer homology* of  $m(L)$  defined in [20]. It bears mentioning that the complex  $(CFL^-(m(L)), \partial^-)$  comes equipped with *Maslov* and *Alexander* gradings, which are then inherited by  $HFL^-(m(L))$ ; however, we will not discuss these gradings further as they play no role in this paper.

Suppose that the link  $L$  has  $l$  components. If  $O_i$  and  $O_j$  lie on the same component of  $L$ , then multiplication by  $U_i$  in  $(CFL^-(m(L)), \partial^-)$  is chain homotopic to multiplication by  $U_j$ , and, so, these multiplications induce the same maps on  $HFL^-(m(L))$  [14, Lemma 2.9]. So, if we label the markings in  $\mathbb{O}$  so that  $O_1, \dots, O_l$  lie on different components, then we can think of  $HFL^-(m(L))$  as a module over  $\mathbb{Z}_2[U_1, \dots, U_l]$ .

Setting  $U_1 = \cdots = U_l = 0$ , one obtains a chain complex  $(\widehat{CFL}(m(L)), \widehat{\partial})$  whose homology we denote by  $\widehat{HFL}(m(L))$ . The latter is a bi-graded vector space over  $\mathbb{Z}_2$ , whose graded Euler characteristic is some normalization of the multivariable Alexander polynomial of  $m(L)$  [20]. If one sets  $U_1 = \cdots = U_k = 0$ , one obtains a chain complex  $(\widetilde{CFL}(m(L)), \widetilde{\partial})$  whose homology we denote by  $\widetilde{HFL}(m(L))$ . The group  $\widehat{HFL}(m(L))$  determines  $\widetilde{HFL}(m(L))$ . Specifically, if we let  $n_i$ , for  $i = 1, \dots, l$ , denote the number of markings in  $\mathbb{O}$  on the  $i$ th component of  $L$ ,

then

$$\widetilde{HFL}(m(L)) = \widehat{HFL}(m(L)) \otimes \bigotimes_{i=1}^l V_i^{\otimes(n_i-1)},$$

where  $V_i$  is a fixed two dimensional vector space [14, Proposition 2.13], and the quotient map

$$j : \widehat{CFL}(m(L)) \rightarrow \widetilde{CFL}(m(L))$$

induces an injection  $j_*$  on homology.

The element  $\mathbf{z}^+(G) \in \mathbf{S}(G)$ , which consists of the intersection points at the upper right corners of the squares in  $G$  containing the markings in  $\mathbb{X}$ , is clearly a cycle in  $(CFL^-(m(L)), \partial^-)$  (and, hence, also in the other chain complexes). If  $T$  is the transverse link in  $(\mathbb{R}^3, \xi_{rot})$  corresponding to the braid obtained from  $G$  as in Figure 2.e, then  $T$  is topologically isotopic to  $L$ , and the image of  $\mathbf{z}^+(G)$  in  $HFL^-(m(T))$  is the transverse invariant  $\theta(T)$  defined in [21]. The images of  $\mathbf{z}^+(G)$  in  $\widehat{HFL}(m(T))$  and  $\widetilde{HFL}(m(T))$  are likewise denoted  $\widehat{\theta}(T)$  and  $\widetilde{\theta}(T)$ , and are invariants of the transverse link  $T$  as well. Moreover, the map  $j_*$  sends  $\widehat{\theta}(T)$  to  $\widetilde{\theta}(T)$ ; in particular,  $\widehat{\theta}(T) = 0$  if and only if  $\widetilde{\theta}(T) = 0$ . The theorem below makes these statements about invariance precise.

**Theorem 3.1** ([21, Theorem 7.1]). *Suppose that  $G$  and  $G'$  are two grid diagrams whose associated braids  $T$  and  $T'$  are transversely isotopic. Then, there is an isomorphism*

$$f_*^o : HFL^o(m(T)) \rightarrow HFL^o(m(T')),$$

*induced by a chain map  $f^o$ , which sends  $\theta^o(T)$  to  $\theta^o(T')$ .*

Here, the superscript “ $o$ ” is meant to indicate that this theorem holds for any of the three versions of link Floer homology described above. In particular, if  $T$  and  $T'$  are two transverse links for which  $\widehat{\theta}(T) \neq 0$  and  $\widehat{\theta}(T') = 0$ , then  $T$  and  $T'$  are not transversely isotopic (the invariant  $\theta(T)$  is always non-zero and non- $U_i$ -torsion in  $HFL^-(m(T))$  [21, Theorem 7.3]). These transverse invariants also behave nicely under negative braid stabilizations.

**Theorem 3.2** ([21, Theorem 7.2]). *Suppose that  $G$  and  $G'$  are two grid diagrams with associated braids  $T$  and  $T'$ , and suppose that  $T'$  is obtained from  $T$  by performing a negative braid stabilization along the  $i$ th component of  $T$ . Then, there is an isomorphism*

$$f_*^- : HFL^-(m(T)) \rightarrow HFL^-(m(T')),$$

*induced by a chain map  $f^-$ , which sends  $\theta(T)$  to  $U_i \cdot \theta(T')$ .*

Since multiplication by  $U_i$  is the same as multiplication by zero on  $\widehat{HFL}$  and  $\widetilde{HFL}$ , we obtain the following corollary.

**Corollary 3.3.** *If  $T'$  is obtained from a transverse braid  $T$  by performing a negative braid stabilization along some component of  $T$ , then  $\widehat{\theta}(T') = \widetilde{\theta}(T') = 0$ .*



4. THE MAP  $\Phi$  AND COMULTIPLICATION

Fix some  $w \in B_n$  and some  $i \in \{1, \dots, n-1\}$ . Figure 4 shows simultaneously a portion of a grid diagram  $G_\beta$  for  $T_{w\sigma_i}$  and the corresponding portion of a grid diagram  $G_\gamma$  for  $T_w$ . The grid diagrams  $G_\beta$  and  $G_\gamma$  are the same except that  $G_\beta$  uses the horizontal curve  $\beta$  while  $G_\gamma$  uses the horizontal curve  $\gamma$ . Let  $k$  denote their common grid number.

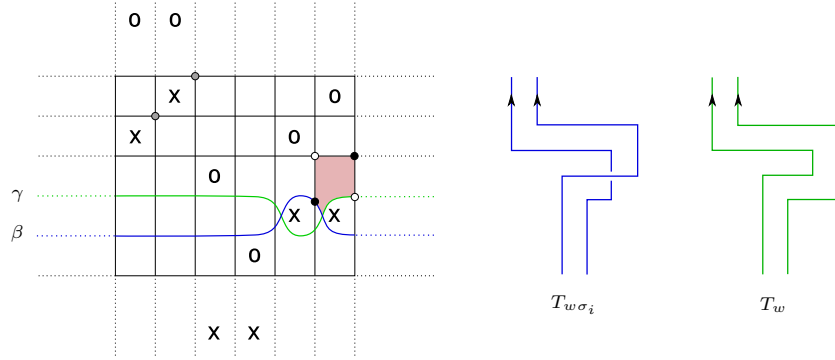


FIGURE 4. A portion of the grid diagrams  $G_\beta$  and  $G_\gamma$ . The cycle  $\mathbf{z}^+(G_\beta)$  is shown as a collection of black and gray dots, while  $\mathbf{z}^+(G_\gamma)$  is represented by the white and gray dots.

For  $\mathbf{x} \in \mathbf{S}(G_\beta)$  and  $\mathbf{y} \in \mathbf{S}(G_\gamma)$ , let  $Pent_{\beta\gamma}(\mathbf{x}, \mathbf{y})$  denote the space of embedded pentagons with the following properties.  $Pent_{\beta\gamma}(\mathbf{x}, \mathbf{y})$  is empty unless  $\mathbf{x}$  and  $\mathbf{y}$  coincide at  $k-2$  points. An element  $p \in Pent_{\beta\gamma}(\mathbf{x}, \mathbf{y})$  is an embedded disk in the torus whose boundary consists of five arcs, each contained in horizontal or vertical circles. We stipulate that under the orientation induced on the boundary of  $p$ , the boundary may be traversed as follows. Start at the component of  $\mathbf{x}$  on the curve  $\beta$  and proceed along an arc contained in  $\beta$  until we arrive at the right-most intersection point between  $\beta$  and  $\gamma$ ; next, proceed along an arc contained in  $\gamma$  until we reach the component of  $\mathbf{y}$  contained in  $\gamma$ ; next, follow the arc of a vertical circle until we arrive at a component of  $\mathbf{x}$ ; then, proceed along the arc of a horizontal circle until we arrive at a component of  $\mathbf{y}$ ; finally, follow an arc contained in a vertical circle back to the initial component of  $\mathbf{x}$ . Let  $Pent_{\beta\gamma}^o(\mathbf{x}, \mathbf{y})$  denote the space of  $p \in Pent_{\beta\gamma}(\mathbf{x}, \mathbf{y})$  for which  $p \cap \mathbb{X} = \text{Int}(p) \cap \mathbf{x} = \emptyset$ .

We construct a map

$$\phi : CFL^-(m(T_{w\sigma_i})) \rightarrow CFL^-(m(T_w))$$

of  $\mathbb{Z}_2[U_1, \dots, U_k]$ -modules as follows. For  $\mathbf{x} \in \mathbf{S}(G_\beta)$ , let

$$\phi(\mathbf{x}) = \sum_{\mathbf{y} \in \mathbf{S}(G_\gamma)} \sum_{p \in Pent_{\beta\gamma}^o(\mathbf{x}, \mathbf{y})} U_1^{O_1(p)} \dots U_k^{O_k(p)} \cdot \mathbf{y}.$$

(This construction is inspired by the proof of commutation invariance in [14, Section 3.1].) The juxtaposition  $p * r$  of any  $p \in Pent_{\beta\gamma}^o(\mathbf{x}, \mathbf{y})$  with any rectangle  $r \in Rect_{G_\gamma}^o(\mathbf{y}, \mathbf{w})$  has precisely

one such decomposition and exactly one decomposition as  $r' * p'$ , where  $r' \in \text{Rect}_{G_\beta}^o(\mathbf{x}, \mathbf{y}')$  and  $p' \in \text{Pent}_{\beta\gamma}^o(\mathbf{y}', \mathbf{w})$ . It follows that  $\phi$  is a chain map and, so, induces a map

$$\Phi : HFL^-(m(T_{w\sigma_i})) \rightarrow HFL^-(m(T_w)).$$

Moreover, it is clear that  $\text{Pent}_{\beta\gamma}^o(\mathbf{z}^+(G_\beta), \mathbf{z}^+(G_\gamma))$  consists only of the shaded pentagon shown in Figure 4, and that  $\text{Pent}_{\beta\gamma}^o(\mathbf{z}^+(G_\beta), \mathbf{y})$  is empty for  $\mathbf{y} \neq \mathbf{z}^+(G_\gamma)$ . Therefore,  $\Phi$  sends  $\theta(T_{w\sigma_i})$  to  $\theta(T_w)$ , proving Theorem 1.1.

The more general comultiplication fact stated in Corollary 1.2 follows from the above result together with the sequence of braid moves depicted in Figure 5. The braid in Figure 5.a represents the transverse link  $T_{hg}$ . The braid in 5.b is obtained from that in 5.a by a mixture of isotopy and positive stabilizations. The braid in 5.c is obtained from that in 5.b by isotopy followed by the introduction of negative crossings. The braid in 5.e is isotopic to the braids in 5.c and 5.d, and represents the connected sum of the transverse links  $T_g$  and  $T_h$  (for the latter statement, see [4]). Therefore, a composition of the maps  $\Phi$  described above (one for each negative crossing introduced in going from 5.b to 5.c) yields a map

$$\mu : HFL^-(m(T_{hg})) \rightarrow HFL^-(m(T_g \# T_h))$$

which sends  $\theta(T_{hg})$  to  $\theta(T_g \# T_h)$ .

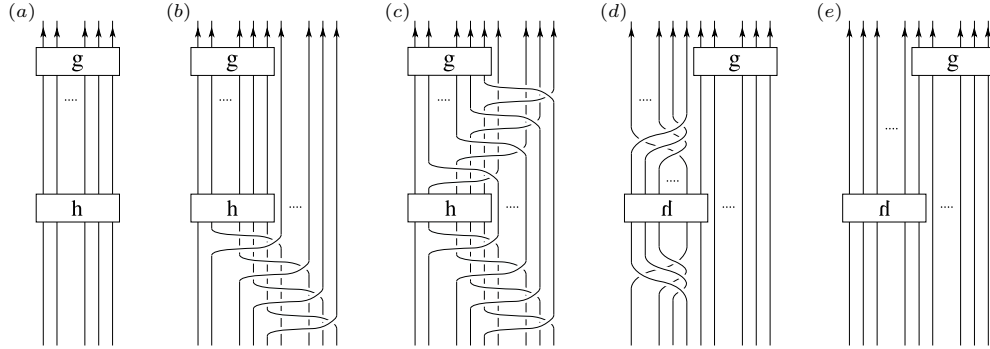


FIGURE 5.  $T_{hg}$  is transversely isotopic to the braid in 5.b, which, after introducing negative crossings (or, equivalently, up to braid isotopy, getting rid of positive crossings) is transversely isotopic to  $T_g \# T_h$ , which is represented by the braid in 5.e.

The map  $\Phi$  has an analogue  $\tilde{\Phi} : \widetilde{HFL}(m(T_{w\sigma_i})) \rightarrow \widetilde{HFL}(m(T_w))$  obtained by counting pentagons which miss both the  $\mathbb{X}$  markings and the  $\mathbb{O}$  markings. It is clear that  $\tilde{\Phi}$  sends  $\tilde{\theta}(T_{w\sigma_i})$  to  $\tilde{\theta}(T_w)$ . Likewise, the comultiplication map  $\mu$  has an analogue

$$\tilde{\mu} : \widetilde{HFL}(m(T_{hg})) \rightarrow \widetilde{HFL}(m(T_g \# T_h))$$

which sends  $\tilde{\theta}(T_{hg})$  to  $\tilde{\theta}(T_g \# T_h)$ .

Suppose that  $T_g \# T_h$  is any connected sum of  $T_g$  and  $T_h$ . In [23], Vértési proves the following refinement of the Kunneth formula described in [20, Theorem 1.4]. (Her proof is actually for the analogous result in knot Floer homology, but it extends in an obvious manner to a proof of the theorem below.)

**Theorem 4.1.** *There is an isomorphism,*

$$\widehat{HFL}(m(T_g \# T_h)) \cong \widehat{HFL}(m(T_g)) \otimes_{\mathbb{Z}_2} \widehat{HFL}(m(T_h)),$$

under which  $\widehat{\theta}(T_g \# T_h)$  is identified with  $\widehat{\theta}(T_g) \otimes \widehat{\theta}(T_h)$ .

Vértési's theorem, used in combination with the comultiplication map  $\tilde{\mu}$ , may be applied to prove Corollary 1.3.

*Proof of Corollary 1.3.* Recall from the previous section that  $\widehat{\theta}(T_w)$  is non-zero if and only if  $\tilde{\theta}(T_w)$  is non-zero. If  $\widehat{\theta}(T_g)$  and  $\widehat{\theta}(T_h)$  are both non-zero, then, by Theorem 4.1, so is  $\widehat{\theta}(T_g \# T_h)$ , and, hence, so is  $\tilde{\theta}(T_g \# T_h)$ . Since  $\tilde{\mu}$  sends  $\tilde{\theta}(T_{hg})$  to  $\tilde{\theta}(T_g \# T_h)$ , this implies that  $\tilde{\theta}(T_{hg})$  is non-zero, and, hence, so is  $\widehat{\theta}(T_{hg})$ .  $\square$

Recall that a braid  $T_g$  is said to be *quasipositive* if  $g \in B_n$  can be expressed as a product of conjugates of the form  $w\sigma_i w^{-1}$ , where  $w$  is any word in  $B_n$ .

**Corollary 4.2.** *If  $T_g$  is a quasipositive braid, then  $\widehat{\theta}(T_g) \neq 0$ .*

*Proof of Corollary 4.2.* If  $g$  is a product of  $m$  conjugates as above, then after resolving the corresponding  $m$  positive crossings, one obtains a braid isotopic to  $I_n$ , the trivial  $n$ -braid. Therefore, a composition of  $m$  of the maps  $\Phi$  sends  $\widehat{\theta}(T_g)$  to  $\widehat{\theta}(I_n)$ . Moreover, one sees by glancing at the grid diagram for  $I_n$  in Figure 6 that  $\tilde{\theta}(I_n) \neq 0$ . Therefore,  $\tilde{\theta}(T_g) \neq 0$  and the same is true of  $\widehat{\theta}(T_g)$ .  $\square$

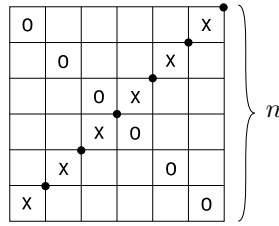


FIGURE 6. A grid diagram  $G_n$  for the trivial braid  $I_n$ . It is straightforward to check that the cycle  $\mathbf{z}^+(G_n) \in \mathbf{S}(G_n)$ , represented by the collection of black dots, is not a boundary in  $\widehat{CFL}(m(I_n))$ .

## 5. FINDING NEW TRANSVERSELY NON-SIMPLE LINKS

In this section, we outline and apply one strategy for using comultiplication (in particular, Corollary 1.3) to generate a plethora of new examples of transversely non-simple link types. Consider the braid words

$$w_1 = a\sigma_1^m b\sigma_1^{-1}c \quad \text{and} \quad w_2 = a\sigma_1^{-1}b\sigma_1^m c$$

in  $B_n$ , where  $a$ ,  $b$  and  $c$  are words in the generators  $\sigma_2, \dots, \sigma_{n-1}$ . The transverse braids  $T_{w_1}$  and  $T_{w_2}$  are said to be related by a *negative flype* and, in particular, represent the same topological link type. If, in addition,  $m$  is odd, or if  $m$  is even and the two strands which cross according to  $\sigma_1^m$  belong to the same component of  $T_{w_1}$ , then  $\mathcal{SL}(T_{w_1}) = \mathcal{SL}(T_{w_2})$ .

Suppose that  $\widehat{\theta}(T_{w_1}) = 0$  and  $\widehat{\theta}(T_{w_2}) \neq 0$ . The idea is to find a word  $h$  in the generators  $\sigma_2, \dots, \sigma_{n-1}$  with  $\widehat{\theta}(T_h) \neq 0$ . Corollary 1.3 would then imply that  $\widehat{\theta}(T_{hw_2}) \neq 0$ . If it is also true that  $\widehat{\theta}(T_{hw_1}) = 0$ , then  $T_{hw_1}$  and  $T_{hw_2}$  are not transversely isotopic although they are topologically isotopic. We would like to find examples which also satisfy  $\mathcal{SL}(T_{hw_1}) = \mathcal{SL}(T_{hw_2})$  (if  $T_{hw_1}$  is a knot, this is automatic) so as to produce topological link types which are not transversely simple. One nice feature of this proposed method, which differs from that in [23], is that there is no reason to believe *a priori* that the link  $T_{hw_1}$  so obtained is composite.

In principle, Corollary 1.3 eliminates half of the work in this scenario – namely, showing that  $\widehat{\theta}(T_{hw_2}) \neq 0$ . In practice, one would like to find examples in which the other half – showing that  $\widehat{\theta}(T_{hw_1})$  is zero – is very easy. To that end, one strategy is to pick an example in which  $T_{w_1}$  is transversely isotopic to a braid which can be negatively destabilized, and to show that the same is true of the braid  $T_{hw_1}$ , which would guarantee that  $\widehat{\theta}(T_{hw_1}) = 0$  by Corollary 3.3. In particular,  $T_{w_1}$  must belong to a topological link type with a transverse representative (that is,  $T_{w_2}$ ) which does not maximize self-linking number, but which cannot be negatively destabilized.

The most well-known such link type is that of the  $(2, 3)$  cable of the  $(2, 3)$  torus knot. In [10], Etnyre and Honda prove the following.

**Proposition 5.1.** *The  $(2, 3)$  cable of the  $(2, 3)$  torus knot has two Legendrian representatives,  $L_1$  and  $L_2$ , both with  $tb = 5$  and  $r = 2$ , for which  $L_1$  is the positive (Legendrian) stabilization of a Legendrian knot while  $L_2$  is not. Moreover,  $L_1$  and  $L_2$  are not Legendrian isotopic after any number of negative (Legendrian) stabilizations.*

That  $L_1$  and  $L_2$  are not Legendrian isotopic after any number of negative stabilizations implies that their transverse pushoffs,  $L_1^+$  and  $L_2^+$ , are not transversely isotopic (yet, they both have  $sl = 3$ ). Moreover, since  $L_1$  is the positive stabilization of a Legendrian knot, its pushoff  $L_1^+$  is transversely isotopic to the negative stabilization of some transverse braid.

Matsuda and Menasco have since given explicit forms for  $L_1$  and  $L_2$  [15]. Figures 7.a and 7.a' depict the rectangular diagrams corresponding to slightly modified versions of these forms (ours are derived from the front diagrams in [16, Figure 6]). Figures 7.b and 7.b' show the rectangular braid diagrams for the transverse pushoffs  $L_1^+$  and  $L_2^+$ , respectively. The braids in 7.c and 7.c' are obtained from those in 7.b and 7.b' by isotoping the red arcs as indicated,

and the braids in 7.d and 7.d' are obtained from those in 7.c and 7.c' after additional simple isotopies and conjugations. The braids in 7.e and 7.e' are obtained from those in 7.d and 7.d' by conjugation, and they are related to one another by a negative flype. Indeed, Figure 7 shows that  $L_1^+$  and  $L_2^+$  are transversely isotopic to the transverse braids  $T_{w_1}$  and  $T_{w_2}$ , respectively, where  $w_1 = a\sigma_1^2b\sigma_1^{-1}c$ ,  $w_2 = a\sigma_1^{-1}b\sigma_1^2c$ ,

$$\begin{aligned} a &= \sigma_4\sigma_3\sigma_5\sigma_6\sigma_4\sigma_5\sigma_5\sigma_6\sigma_4\sigma_5\sigma_7\sigma_6\sigma_5^{-1}\sigma_4^{-1}\sigma_3^{-1}\sigma_2\sigma_3\sigma_3\sigma_4\sigma_5\sigma_4^{-1}\sigma_3^{-1}\sigma_2^{-1}, \\ b &= \sigma_5\sigma_6\sigma_7\sigma_6^{-1}\sigma_5^{-1}\sigma_4^{-1}\sigma_6^{-1}\sigma_5^{-1}\sigma_4^{-1}\sigma_3\sigma_4\sigma_5\sigma_2\sigma_3\sigma_4\sigma_4\sigma_5\sigma_6\sigma_5^{-1}\sigma_4^{-1}\sigma_3^{-1}\sigma_2^{-1}, \text{ and} \\ c &= \sigma_7^{-1}\sigma_6^{-1}\sigma_5^{-1}. \end{aligned}$$

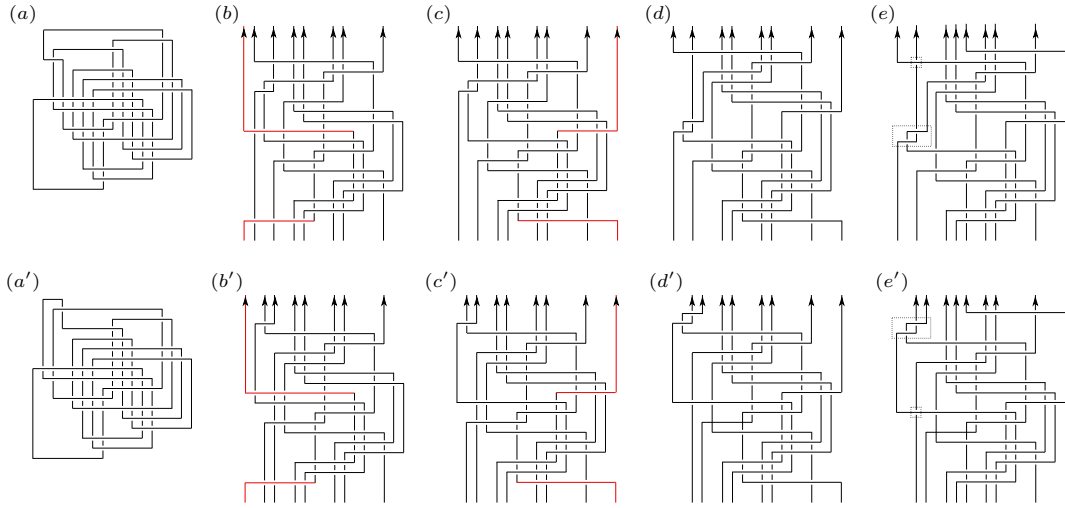


FIGURE 7. On the top, the rectangular diagrams for  $L_1$  and its transverse pushoff  $L_1^+$ . On the bottom, those for  $L_2$  and  $L_2^+$ . The circled regions in 7.e and 7.e' indicate that  $L_1^+$  and  $L_2^+$  are transversely isotopic to braids related by a negative flype.

According to Proposition 5.1,  $T_{w_1}$  is transversely isotopic to a braid which can be negatively destabilized. Figure 8 shows a sequence of transverse braid moves which demonstrates that the same is true of  $T_{hw_1}$  for any word  $h \in B_8$  in the generators  $\sigma_3, \dots, \sigma_6$ . The braid in Figure 8.a is obtained from that in 8.a by isotoping the red and blue arcs as shown. The braid in 8.c is related to that in 8.b by an exchange move at the circled crossings in 8.b. The braid in 8.d is obtained from that in 8.c by isotopy of the red, blue and green arcs. The braid in 8.e is obtained from that in 8.d after the indicated isotopy of the yellow, orange and purple arcs. An exchange move at the circled crossings in 8.e produces the braid in 8.f. The braid in 8.g is obtained from that in 8.f by isotoping the red arc as shown. The braid in 8.h is obtained from that in 8.g after an isotopy of the blue, green and purple arcs as shown. An exchange move at the circled crossings in 8.h, followed by the indicated isotopy of the red arc produces the braid in 8.i. Finally, the braid in 8.j is obtained from that in 8.i by an exchange move at the circled crossings in 8.i, followed by the indicated isotopy of the blue arc. Note that the braid

in 8.j may be negatively destabilized at the circled crossing. The essential point here is that the region of the braid in 8.a corresponding to the word  $h$  is not affected by this combination of isotopies and exchange moves.

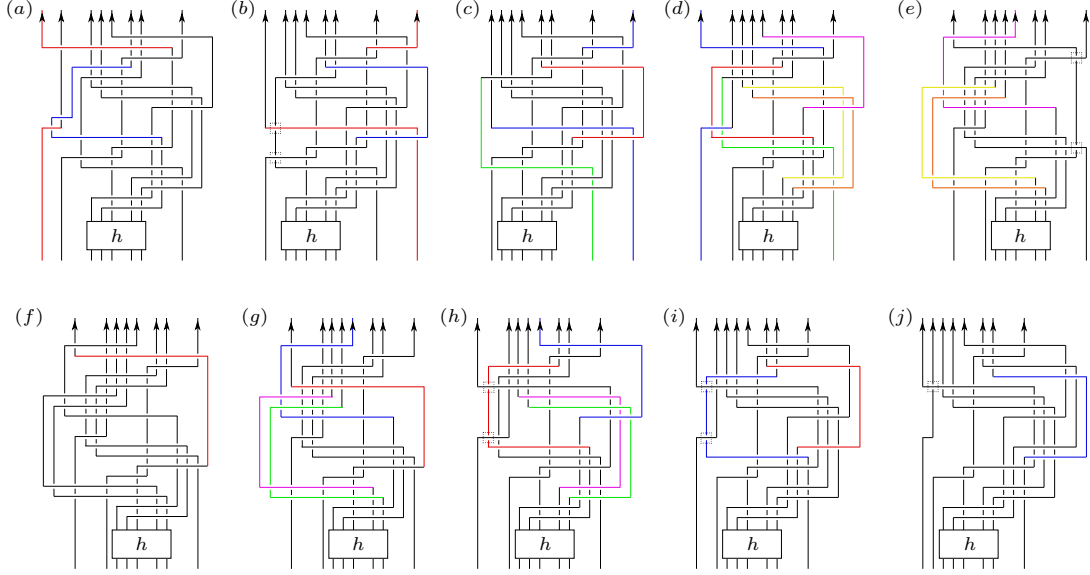


FIGURE 8. Figure 8.a shows a rectangular braid diagram for  $T_{hw_1}$ . After a sequence of braid isotopies and exchange moves, we obtain the braid in 8.j, which can be negatively destabilized.

To sum up: since  $\widehat{\theta}(T_{w_2}) \neq 0$  (see [16]), we have proven that for any  $h \in B_8$  which is 1) a word in the generators  $\sigma_3, \dots, \sigma_6$  and for which 2)  $\widehat{\theta}(T_h) \neq 0$ , it is the case that  $\widehat{\theta}(T_{hw_1}) = 0$  while  $\widehat{\theta}(T_{hw_2}) \neq 0$ . It follows that the transverse braids  $T_{hw_1}$  and  $T_{hw_2}$  are not transversely isotopic though they are topologically isotopic. If, in addition, 3)  $h$  is such that the two strands of  $T_{hw_1}$  which cross according to the string  $\sigma_1^2$  belong to the same component of  $T_{hw_1}$ , then  $\mathcal{SL}(T_{hw_1}) = \mathcal{SL}(T_{hw_2})$ ; that is, the topological link type represented by  $T_{hw_1}$  is transversely non-simple.

There are infinitely many choices of  $h$  which meet criteria 1) - 3) above. In order to give such an  $h$ , we first prove the following.

**Lemma 5.2.** *For  $1 \leq j \leq k$  and  $0 \leq l \leq k - j$ , consider the map  $\psi_{j,k,l} : B_j \rightarrow B_k$  which sends  $\sigma_i$  to  $\sigma_{i+l}$ . If  $g$  is a word in  $B_j$  for which  $\widehat{\theta}(T_g) \neq 0$ , and  $h = \psi_{j,k,l}(g)$ , then  $\widehat{\theta}(T_h) \neq 0$  as well.*

See Figure 9 for a pictorial depiction of the map  $\psi_{j,k,l}$ .

*Proof of Lemma 5.2.* If  $h = \psi_{j,k,l}(g)$ , then the braid  $T_h$  is easily seen to be connected sum of  $T_g$  with the trivial braids  $I_{k-j-l+1}$  and  $I_{l+1}$ . We know, from the proof of Corollary 4.2, that  $\widehat{\theta}(I_n) \neq 0$  for any  $n \geq 1$ . Lemma 5.2 therefore follows from Theorem 4.1.  $\square$

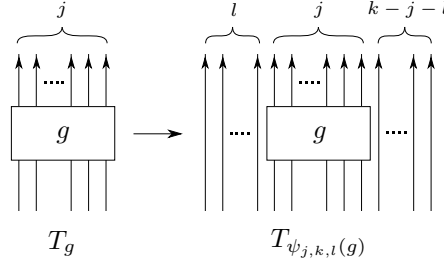


FIGURE 9. On the left, the  $j$ -braid  $T_g$ . On the right, the  $k$ -braid  $T_{\psi_{j,k,l}(g)}$ .

It follows from Corollary 4.2 and from Lemma 5.2 that  $h = \psi_{4,8,3}(g)$  satisfies criteria 1) and 2) above as long as  $T_g$  is a quasipositive 4-braid. Let  $h = \psi_{4,8,3}(g)$  for

$$g = \sigma_3 \sigma_2 \sigma_3 \sigma_1 \sigma_2 \sigma_3.$$

It is easy to check that  $h^n$  also satisfies criterion 3) (as well as criteria 1) and 2), of course) for all  $n \geq 0$ .

**Corollary 5.3.** *The topological link types represented by  $T_{h^n w_1}$  are transversely non-simple for all  $n \geq 0$ . When  $n$  is even,  $T_{h^n w_1}$  is a knot; otherwise,  $T_{h^n w_1}$  is a 3-component link.*

Below, we prove that most of the links in Corollary 5.3 are prime. Note that  $T_{h^n w_1}$  is obtained from  $T_{w_1}$  by performing  $n$  positive half twists of strands 4 - 7 in the region of  $T_{w_1}$  where we would insert the word  $h^n$ . For  $n = 2m$ , this amounts to adding  $m$  positive full twists, which can also be accomplished by performing  $-1/m$  surgery on an unknot  $U$  encircling strands 4 - 7 of  $T_{w_1}$  in the corresponding region. See Figure 10.

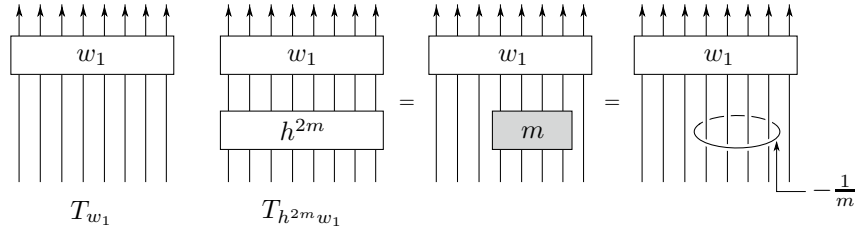


FIGURE 10.  $T_{h^{2m} w_1}$  is obtained from  $T_{w_1}$  by performing  $m$  positive full twists of strands 4 - 7, or, equivalently, by performing  $-1/m$  surgery on the unknot shown on the right.

A *SnapPea* computation [24] shows that the complement of the link  $T_{w_1} \cup U$  is hyperbolic. Thurston's celebrated Dehn Surgery Theorem then implies that all but finitely many Dehn fillings of the boundary component corresponding to  $U$  are hyperbolic as well [22]. In turn, this implies that the link  $T_{h^{2m} w_1}$  is hyperbolic, and, hence, prime for all but finitely many  $m$ . This argument can be repeated to show that the links  $T_{h^{2m+1} w_1}$  are also prime for all but finitely many  $m$ . The lemma below sums this up.

**Lemma 5.4.** *The links  $T_{h^n w_1}$  are prime for all but finitely many values of  $n$ .*

## REFERENCES

- [1] K. Baker, J.B. Etnyre, and J. Van Horn-Morris. Fibered transverse knots and the bennequin bound. 2008, math.GT/0803.0758.
- [2] J. A. Baldwin. Comultiplicativity of the Ozsváth-Szabó contact invariant. *Math. Res. Lett.*, 15(2):273–287, 2008.
- [3] D. Bennequin. Entrelacements et équations de Pfaff. *Astérisque*, 107-108:87–161, 1983.
- [4] J.S. Birman and W.W. Menasco. Studying links via closed braids IV: composite links and split links. *Inv. Math.*, 102(1):115–139, 1990.
- [5] J.S. Birman and W.W. Menasco. Stabilization in the braid group II: Transversal simplicity of knots. *Geom. Topol.*, 10:1425–1452, 2006.
- [6] Y. Eliashberg. Legendrian and transversal knots in tight contact 3-manifolds. In *Topological methods in modern mathematics*, pages 171–193. Publish or Perish, 1993.
- [7] J. Epstein, D. Fuchs, and M. Meyer. Chekanov-Eliashberg invariants and transverse approximations of Legendrian knots. *Pac. J. Math.*, 201(1):89–106, 2001.
- [8] J. B. Etnyre. Transversal torus knots. *Geom. Topol.*, 3:253–268, 1999.
- [9] J. B. Etnyre and K. Honda. Knots and contact geometry I: torus knots and the figure eight knot. *J. Symp. Geom.*, 1(1):63–120, 2001.
- [10] J. B. Etnyre and K. Honda. Cabling and transverse simplicity. *Ann. of Math.*, 162(3):1305–1333, 2005.
- [11] K. Kawamuro. Connect sum and transversely non-simple knots. *Math. Proc. Cambridge Philos. Soc.*, to appear, 2008.
- [12] T. Khandhawit and L. Ng. A family of transversely nonsimple knots. 2008, math.GT/0806.1887.
- [13] C. Manolescu, P. Ozsváth, and S. Sarkar. A combinatorial description of knot Floer homology. 2006, math.GT/0607691.
- [14] C. Manolescu, P. Ozsváth, Z. Szabó, and D. Thurston. On combinatorial link Floer homology. 2007, math.GT/0610559.
- [15] W. W. Menasco and H. Matsuda. An addendum on iterated torus knots (appendix). 2006, math.GT/0610566.
- [16] L. Ng, P. Ozsváth, and D. Thurston. Transverse knots distinguished by knot Floer homology. *J. Symp. Geom.*, 6(4):461–490, 2008.
- [17] L. Ng and D. Thurston. Grid diagrams, braids, and contact geometry. 2009, math.GT/0812.3665.
- [18] S. Orevkov and V. Shevchishin. Markov Theorem for Transverse Links. *J. Knot Theory Ram.*, 12(7):905–913, 2003.
- [19] P. Ozsváth and A. Stipsicz. Contact surgeries and the transverse invariant in knot floer homology. 2008, math.GT/0803.1252.
- [20] P. Ozsváth and Z. Szabó. Holomorphic disks, link invariants, and the multi-variable Alexander polynomial. *Algebr. Geom. Topol.*, 8:615–692, 2008.
- [21] P. Ozsváth, Z. Szabó, and D. Thurston. Legendrian knots, transverse knots, and combinatorial Floer homology. 2008, math.GT/0611841.
- [22] W. Thurston. *The geometry and topology of three-manifolds*. Princeton, 1979.
- [23] V. Vértesi. Transversely non-simple knots. *Algebr. Geom. Topol.*, 8:1481–1498, 2008.
- [24] J. Weeks. SnapPea. <http://www.geometrygames.org/SnapPea/index.html>.
- [25] N. Wrinkle. The Markov theorem for transverse knots. 2002, math.GT/0202055.

DEPARTMENT OF MATHEMATICS, PRINCETON UNIVERSITY, PRINCETON, NJ 08544-1000

*E-mail address:* baldwinj@math.princeton.edu